Biotribology 5 (2016) 31–43

Contents lists available at ScienceDirect

Biotribology

journal homepage: http://www.elsevier.com/locate/biotri

Lotus effect in wetting and self-cleaning

Mingqian Zhang, Shile Feng, Lei Wang, Yongmei Zheng *

Key Laboratory of Bio-Inspired Smart Interfacial Science and technology of Ministry of Education, School of Chemistry and Environment, Beihang University, Beijing 100191, P. R. China

ARTICLE INFO

Article history:
Received 22 July 2015
Received in revised form 30 August 2015
Accepted 30 August 2015
Available online 3 September 2015

Keywords:
Lotus effect
Self-cleaning
Superhydrophobic
Roughness
bio-inspired
Hierarchical structure

ABSTRACT

Self-cleaning surfaces based on lotus effect with a very high static water contact angle greater than 160° and a lower roll-off angle have been successfully studied by researchers and applied in fields of self-cleaning windows, windshields, exterior paints for buildings and navigation of ships, utensils, roof tiles, textiles, solar panels, and applications requiring a reduction of drag in fluid flow, e.g. in micro −/nanochannels. In this feature article, we summarize recent research progress and synthesis technologies about the design and fabrication of self-cleaning surfaces. We hope that, this review article should provide a useful guide for the development of self-cleaning surfaces.

1. Introduction

Over thousands of years of natural selection, living organisms including all plants and animals on our earth are evolutionarily optimized functional systems. One of their most fascinating properties is the ability of self-cleaning which means that the surfaces can repel contaminants such as solid particles, organic liquids, and biological contaminants by the action of rolling-off water drops. This kind of self-cleaning surfaces has both the ability of superhydrophobicity and self-cleaning properties, and with lotus leaf as the typical representative, therefore is known as "Lotus effect". [1–8] During the past few decades, a large number of studies have been conducted to a full understanding of the functions, structures, and principles of self-cleaning surfaces. The conclusion recognized that the requirements for a self-cleaning surface are superhydrophobic property with a very high static water contact angle greater than 160°, and a very low roll-off angle, i.e. the minimum inclination angle necessary for a droplet to roll off the surface. [3,9] By now, many different synthesis technologies have been developed to design and fabricate self-cleaning surfaces. [10–14] Today, a great variety of self-cleaning surfaces based on lotus effect have also been commercialized with the range from window glasses to solar cell panels. [15–18].

In this feature article, we summarize recent research progress in the field of bio-inspired self-cleaning surfaces based on lotus effect about the mechanism, fabrication, and application. At first, we discuss the impact of multi-scale roughness and low energy waxes on the self-cleaning property, respectively. And in the next section, we briefly summarize and discuss the conventional self-cleaning methods. We categorize recent progress in this area into two aspects as the technologies of constructing hierarchical roughness structure onto the hydrophobic surfaces and the technologies of coating low energy materials onto the rough surfaces. Furthermore, the review introduces briefly the application prospects and challenges of self-cleaning surfaces based on lotus effect. We hope, this review article should provide a useful guide for the development of self-cleaning surfaces.

2. Lotus effect—the self-cleaning property of lotus leaf surface

As we known, the lotus leaf has long been regarded as the symbol of sacred purity in China, and sang praises by number of poets. The verse of "the lotus and leaves all over the pond, and breeze blows beads roll down" described that water drops falling onto the leaves can bead up and roll off, with washing dirt from the lotus leaves so that they are self-cleaning, which is known as "Lotus effect". This phenomenon of lotus effect is not restricted to lotus leaf surface. Some other plants and insects also evolved self-cleaning surfaces. For instance, the droplets of water on the rice leaves [19,20], *Salvinia molesta* [21,22], butterfly wings, fish scales, shark skin [20,23] and mosquito eyes [24] (as shown in Fig. 1) can roll off following a preferential direction dictated by the structural features.

For an understanding of the functions, structures, and principles of various objects that exhibit self-cleaning found in living nature, a large

* Corresponding author.
E-mail address: zhengym@buaa.edu.cn (Y. Zheng).

http://dx.doi.org/10.1016/j.biotri.2015.08.002

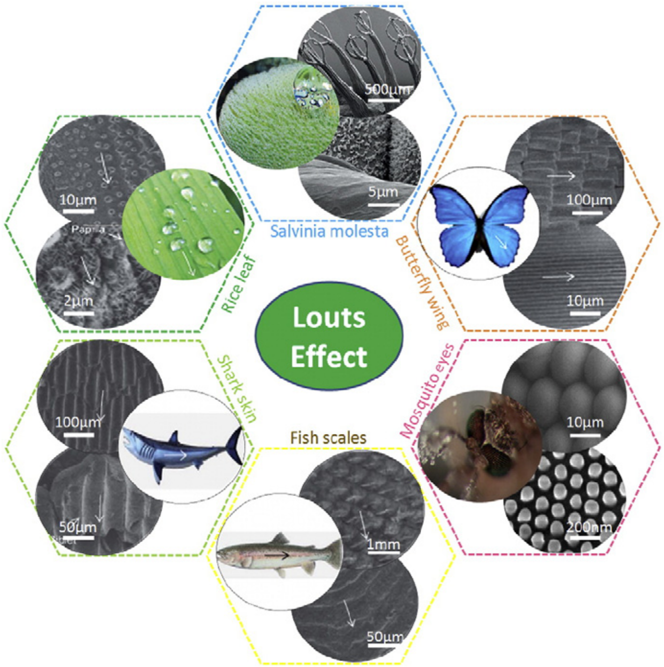

Fig. 1. The typical self-cleaning surfaces in nature and their SEM images.

number of studies have been conducted onto surface structure and chemical composition.

2.1. Effect of the hierarchical roughness of the lotus leaf surfaces

In order to reveal the roles of the roughness and waxes covered over the entire surface of lotus leaf on the self-cleaning property, many scientific research workers carried out extensive researches. Neinhaus and Barthlott investigated nearly 300 kinds of plant leaf surface, and indicated that this self-cleaning property is caused by both the rough structure and the hydrophobic epicuticular waxes. [2,3].

In 2002, Jiang reported a new discovery, indicating that, there are fine branch-like nanostructures covered on the every micro-papilla of the lotus leaf surface. [25] And this kind of micro- and nanohierarchical composite structure of the lotus leaf surface realized superhydrophobic and low adhesive performance.

Fig. 2b shows a typical scanning electron microscopy image of a lotus leaf. We can see that lotus leaf surfaces possess randomly distributed micro-papillae with diameters ranging from 5 μm to 9 μm. Fig. 2c shows a high-resolution SEM image of a single papilla which proves that on each papilla and the gaps of surface among papillae, fine branch-like nanostructures with diameter of approximately 120 nm have been observed. These nanostructures would effectively prevent the underside of leaf from being wetted. The multi-scale structures combined with micro-papillae and nano-hairs provide air pocket formation, thus, water can interact with only the peaks of the roughness surface instead of by wetting the entire surface, both the peaks and valleys. In this case, the apparent contact angle, θ_{CB}, is given by the Cassie–Baxter (noted as CB) equation for wetting on composite surfaces made of the solid and air, [26]

$$\cos\theta_{CB} = f_s\cos\theta + f_s - 1 \tag{1}$$

where f_s is the fraction of projected planar area of the drop in contact with the solid. In the limit of $f_s \rightarrow 0$, the macroscopic contact angle θ_{CB} approaches 180°, leading to superhydrophobic behavior. That is to say, the multi-scale structures result in the lowest contact area between lotus leaf surfaces and water droplets. And drops in the Cassie-Baxter state can easily roll because of low resistance from the air pockets. [27,28] Therefore, we can say that, this kind of micro- and nano- hierarchical structure amplifies the apparent contact angle and is responsible for the rolling behavior of the drops.

Cheng and Rodak et al. studied the influence of micro- and nano-scale structures on the wetting behavior of lotus leaves by separated the effects of nano-scale features from micro-scale roughness on the wetting behavior. [29] They annealed the leaves for 1 h at 150 °C, and examined by SEM (as shown in Fig. 2d). The result showed that all the nano-scale hair-like structures from the leaf were removed, leaving behind only micro-structure surface. The wax present on the surface of the untreated and annealed lotus leaves does not appear to undergo any gross chemical change, based on the IR data. For comparison, the static water contact angles on the untreated lotus leaf, annealed lotus leaf and smooth of carnauba wax were measured. And the result values were 142.4 ± 8.6°, 126.3 ± 6.2°, and 74.0 ± 8.5°. These results indicate that the carnauba wax is not very hydrophobic because of its many hydrophilic functional groups, which is also consistent with Wagner's conclusion. [30] Thus, the micro-scale roughness on lotus surfaces is effective in increasing the static contact angle, and the presence of the nano-scale hair-like structure is responsible for the additional increase of 16° in contact angle from 126° to 142°.

In addition, while water drops placed on the lotus leaves roll off at the slightest incline, the same size drops become sticky drops on the annealed leaf, adhering to the surface even when the leaf is tilted 90°

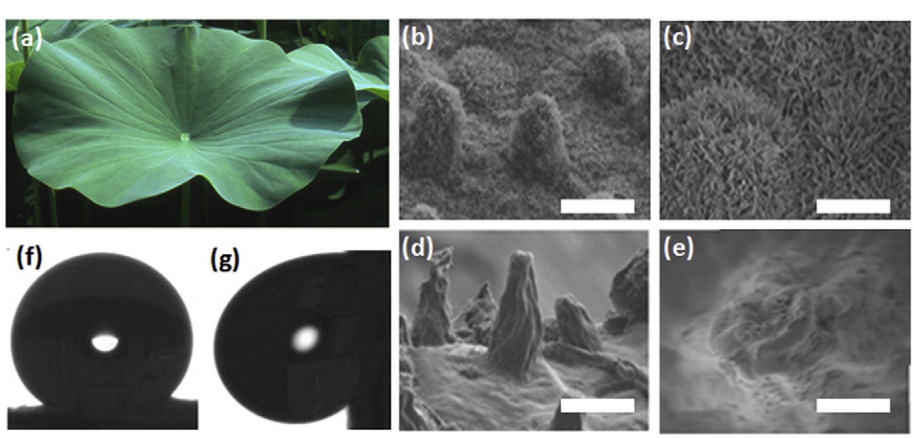

Fig. 2. Image and SEM images of lotus leaf surface. (a) A fresh lotus leaf in nature (b) the micro-structure of lotus leaf (c) the nano-structure of lotus leaf (d) the micro-structure of annealed lotus leaf (e) the nano-structure of annealed lotus leaf (f) a droplet placed on an untreated lotus leaf, and (g) a droplet placed on an annealed lotus leaf, then tilted to an angle of 90°. (Scale bar: (b and d) 10 μm, (c and e) 3 μm).

(as shown in Fig. 2f) or turned upside down. It means that the nano-scale hair structure of lotus leaf is conducive to reduce the surface adhesion of lotus leaf. The rolling motion more efficiently cleans the surface without dirt left than the sliding motion that occurs at lower contact angles. Therefore, this phenomenon proves the critical role of nano-scale hair structure in making self-cleaning property of lotus leaves.

In summary, for the hierarchical roughness structure of the lotus leaf surfaces, air pockets forming inside the grooves underneath the liquid reduce the contact area between the liquid and the surface, resulting in the reduction of contact angle hysteresis, tilt angle, and adhesive force. The combination of the micro-scale mounds and the nano-scale hair-like structures is responsible for superhydrophobicity and self-cleaning properties and the nano-scale hair-like structure plays a more important role in the aspect of self-cleaning property of the lotus leaf.

2.2. Effect of the epicuticular waxes covered across the lotus leaf surfaces

Furthermore, hydrophobic three-dimensional (3D) epicuticular waxes were found on the surface of the leaf, which are thought responsible for the lotus leaf's water repellency and self-cleaning property. Although, Wagner [30] has concluded the carnauba wax is not very hydrophobic because of its many hydrophilic functional groups. However, epicuticular waxes are made from a mixture of biopolymers that have and appear to be very inhomogeneous in structure and composition, therefore, show a variability degree of wettability. [31–33] And it must be noted that, most of epicuticular waxes including that of lotus leaf are hydrophobic because of their low surface energy hydrocarbon compounds. If the wax present on the surface is removed by washing with acetone, the contact angle is dramatically reduced. [34,35] Only the liquid which has a surface tension equal to or lower than the critical surface tension of a solid can spread on this solid surface. So, on the low energy surface, since the force that keeps the water in contact with the solid is lower, the water will keep as a spherical droplet, which leads a lower wet area and lower the roll-off angle(as shown in Fig. 3a), comparing with high energy surface(as shown in Fig. 3b). Thus, the superhydrophobic state is considered to be generated by the combination of a hierarchical surface structure that traps air beneath a water droplet and the hydrophobicity of the surface wax.

Another interesting observation of Fürstner et al. [36] was that despite the missing structure of the wax crystals, the water contact angle of the lotus replica was the highest of all the replicates, indicating that the microstructure formed by the papillae alone is already optimized with regard to water repellency. Otherwise, recent studies and experiments have demonstrated that is possible to obtain superhydrophobic surfaces on hydrophilic substrates by tuning the roughness and morphology of surface. Several superhydrophobic surfaces have been obtained on hydrophilic materials (i.e. water contact angle of flat surface <90°) by inducing an adequate roughness. [11,17,37–39] Thus, we conclude that the hydrophobic and self-cleaning properties of lotus leaf are caused by both the rough structure and the hydrophobic epicuticular waxes, and the intrinsic hierarchical rough structure is a more important key role of them.

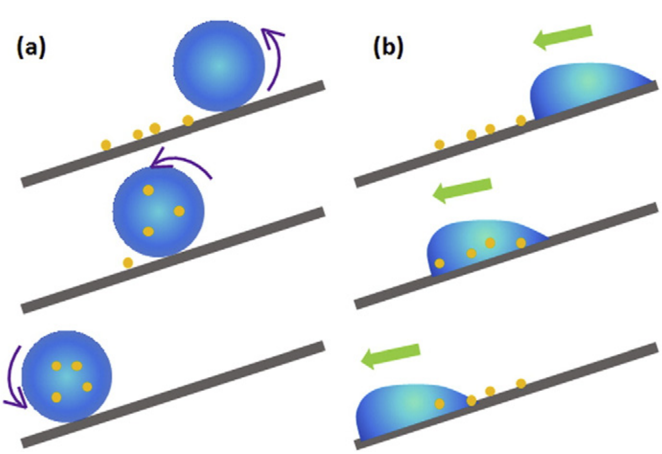

Fig. 3. Self-cleaning of a low energy superhydrophobic surface. (a) A drop with a very high contact angle washes out contamination particles, (b) while a drop with low contact angle does not clean the surface.

3. Fabrication methods of self-cleaning surfaces

Self-cleaning technology has developed since the late 20th century, and some achievements have led to practical application. [40–44] As we know that, the self-cleaning property of lotus leaf is based on the combine of its roughness surface and low surface energy wax. [23,45,46] Therefore, we can obtain two ideas for preparation of self-cleaning surfaces inspired by the Lotus effect but not constrained by lotus leaf structure. First, to construct micro-/nanocomposite hierarchical structure on an initial hydrophobic surface, and second, to modify low surface energy materials on the micro-/nanocomposite hierarchical structure surface. In this section, we mainly review preparation methods of self-cleaning surfaces with micro-/nanocomposite hierarchical and low surface energy.

It should be pointed out that, some technologies such as deposition [47–54] without controlling the morphology of sample, are one-step preparation method of roughness surface with different sizes of micro-/nanocomposite structure directly; while some technologies include two or more steps: preparation of the micro-structure and preparation of nanometer structure. These technologies can be employed dependently, or coupling with others to fabricated the self-cleaning surfaces.

3.1. Techniques to fabricate micro-/nanostructure

3.1.1. Lithography

In recent years, lithography has proved to be useful and become the widely employed technique for the synthesis of self-cleaning surface with controlled micro-/nanocomposite structures. It includes photo, E-beam, X-ray, and soft lithography. [14,55–61].

Fürstner and Barthlot [36] fabricated self-cleaning silicon wafer specimens with different regular arrays of spikes(as shown in Fig. 4a) by X-ray lithography. These silicon samples could be cleaned almost completely from artificial particulate contaminations by a fog consisting of water droplets. Bhushan and Jung [62] produced silicon surfaces patterned with pillars of two different diameters and heights with varying pitch values using photolithography(as shown in Fig. 4b). Then, a self-assembled monolayer (SAM) of 1,1,—2,2,-tetrahydroperfluorodecyltrichlorosilane (PF3) was deposited on the sample surfaces using vapor phase deposition technique to change the surface form initially hydrophilic to hydrophobic. A water droplet in state of the composite interface shows significantly less hysteresis and tilt angles compared to a water droplet in state of the homogeneous interface due to low resistance from the air pockets.

In particular, this technique can allow the precise control of the structure on the surface of a work piece, and apply for large area of periodic micro/nanopatterns. In other words, surfaces patterned with different shapes and different sizes can be prepared by this route. The advantage of lithography is that the template is easy to be fabricated and can be used many times, and, the obtained structures of surfaces are various. However, the process of lithography needs a long molding cycle with a high cost and it is liable to produce defects.

3.1.2. Anodization

Anodization [63–66] is a kind of metal surface treatment in which the surface of a metal and its alloy form an oxide film through the impressed anodic current in the electrolyte solution. It often serves as a material protection technology.

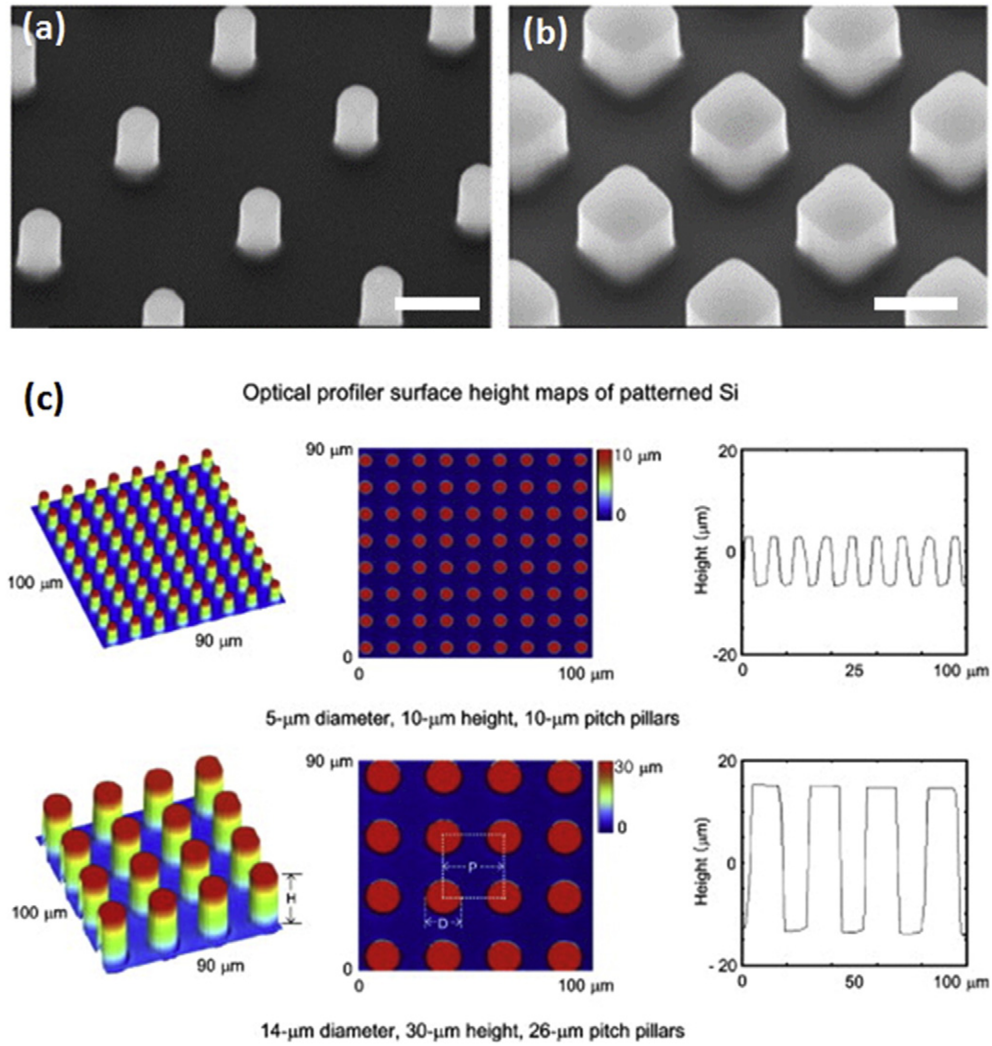

Fig. 4. (a) SEM images of microstructured waterrepellent silicon surfaces with regular patterns of spikes. (b)Surface height maps and 2D profile of the patterned Si surfaces using an optical profiler. The diameter and height of the pillar are D and H, respectively. The pitch of the pillars is P. (Scale bar: (a) left 1 μm, right 2 μm).

Kim and Hwang et al. [67] fabricated robust and large-area alumina nanowire structures with superhydrophobic property by an inexpensive single-step anodization process that can routinely create arbitrary three-dimensional shapes, as shown in Fig. 5. Water droplets rolled easily without any trace on the surface by tilting the substrate slightly.

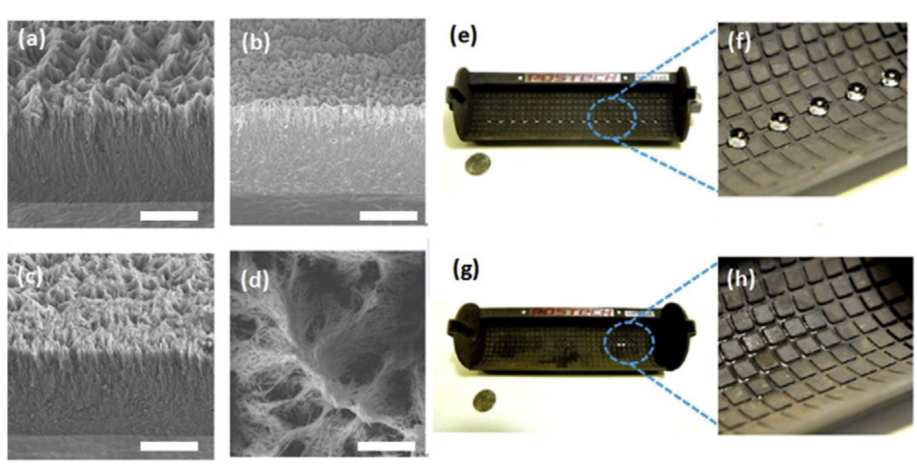

Fig. 5. SEM images showing the thickness of the anodized Al surface after differing anodization times, and HDFS coated surface. (a) Cross-section view of anodized Al (anodization time: 10 min). (b) Cross-section of anodized Al (anodization time: 1 h). (c) Cros-section of anodized Al with HDFS. (d) Top view of anodized Al with HDFS. (c, d) Anodization time: 10 min. (Scale bar: (a − c) 10 μm, (d) 1 μm).

3.1.3. Etching

Etching including plasma etching [52,68,69], laser etching [13,70,71], and chemical etching [13,52,53,72–74], is a straightforward and effective way of fabricating rough structure surface by etching surface with corrosive gas plasma or laser.

Hatzikiriakos et al. [75] fabricated certain dual scale roughness structures by treated different metal alloys initially shown superhydrophilic behaviors with femtosecond laser irradiation. As a result, these surfaces become nearly superhydrophobic with contact angles in the vicinity of 150° and even superhydrophobic with contact angles above 150° over time. The contact angle hysteresis was found to lie between 2 and 6°, which indicated that the surfaces have predominant self-cleaning property. Breedveld and coworkers [76] obtained a roll-off superhydrophobic cellulose paper by domain-selective etching of amorphous portions of the cellulose in oxygen plasma and subsequently coating the etched surface with a thin fluorocarbon film deposited via plasma-enhanced chemical vapor deposition using pentafluoroethane as a precursor. The contact angle was up to 166.7°, and the contact angle hysteresis was 3.4°. Kwon et al. formed micro-scaled textures on a silicon surface using deep reactive etching and nano-scaled textures on the micro-scaled textures using XeF_2 etching, [77] as shown in Fig. 6. The XeF_2 etching could provide uniform roughness at nano-scale on the surface, but the etching time should be carefully controlled to avoid over-etching. The etched surface was coated with a heptadecafluoro-1, 1, 2, 2-tetrahydrodecyl trichlorosilane (HDFS) self-assembled monolayer (SAM) to prompt large intrinsic contact angles and therefore the CB superhydrophobicity. In the droplet bouncing test, the droplet that landed on the surface with double-layered roughness would always find the CB state energetically favorable, and it could bounce back from the surface, showing great superhydrophobicity.

Robert et al. fabricated tunable hydrophobic/hydrophilic flexible Teflon nanocone array surfaces by the oxygen plasma etching of a colloidal monolayer of polystyrene beads on a Teflon film. [78] As shown in Fig. 7, the nanocone array surfaces could be made superhydrophobic with a maximum contact angle of 160° by the further modification of the AuNPs with an octadecanethiol ($C_{18}SH$) monolayer.

Xu [79] reported that a superhydrophobic surface on an aluminum substrate was fabricated by one-step electrochemical etching which was applied as an effective technique using the sodium chloride(NaCl) aqueous solution containing fluoroalkylsilane as the electrolyte. The resulting superhydrophobic surfaces showed a static water contact angle of 166° and a tilting angle of about 1°. The water was dropped to the upper side of the surface by a plastic dropper, as shown in Fig. 8. Subsequently, it fell on the superhydrophobic surfaces bead up and rolls off freely by taking away graphite powder on the surface.

Etching technology, with merits such as high selectivity and rapid, is an effective preparation method of rough structure surface. However, it has a heavy cost and could not be employed to fabricate large scale superhydrophobic surface.

3.1.4. Template replica

Template replica method [80–83] is generally an effective, fast, very low-cost, and reproducible way to obtain rough structure, which has been widely used in the preparation of self-cleaning surface.

By using the nanocasting method, Yuan et al. [84] fabricated a superhydrophobic film from a natural lotus leaf on polyvinyl chloride (PVC) in two steps (as shown in Fig. 9): (i) achieving a negative surface of a lotus leaf using polydimethylsiloxane (PDMS) (as shown in Fig. 9c-d), and (ii) casting PVC over a negative template (as shown in Fig. 9e-f). Here the water contact angle reached ~157° (as shown in Fig. 9h) with a roll-off angle of 3°, showing superhydrophobicity and self-cleaning performance.

Zheng et al. [85] successfully fabricated an artificial PDMS polymer surface by mimicking taper-ratchets from ryegrass leaf using a two-step template replica method. The surfaces display a robust property of directional water shedding-off. As shown in Fig. 10, when external vibrations are executed on polymer surfaces, the drops achieve a unidirectional self-shedding along the oriented direction of tips of taper-ratchets, because asymmetric retention forces are formed in the contrasting oriented directions.

This method has the merits including simple, accurate, effective, low cost and large-scale preparation. But while it has several fatal limits including that the template has a short service life generally, is not readily applied to create complex shaped structures, and has low mechanical strength facing external pressure.

3.2. Techniques to fabricate superhydrophobic coating

There are several ways to modify the chemistry of a surface including sol–gel, dip coating, self-assembly, electrochemical and chemical/physical vapor deposition.

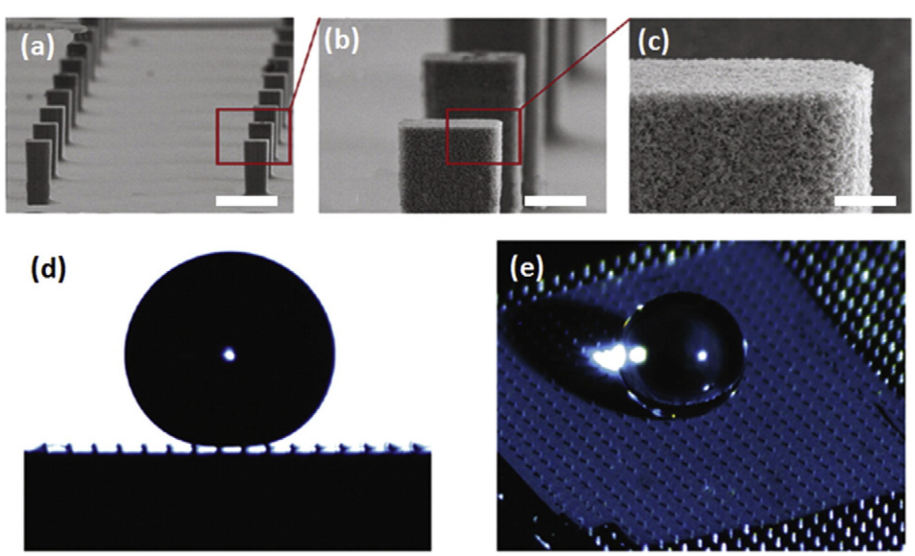

Fig. 6. Droplet on the fabricated micro/nano roughened hierarchical surface. (a-c) Nano-scaled roughness etched by XeF_2 gas that conformally covers the micro-scale array of pillars fabricated through deep reactive etching. (d-e) Droplet sitting on the double roughness with the value of the pillar spacing to width ratio at 7.5, supported by only several pillars. The contact angle at this state is 173°. (Scale bar: (a) 50 μm, (b) 10 μm, and (c) 2 μm).

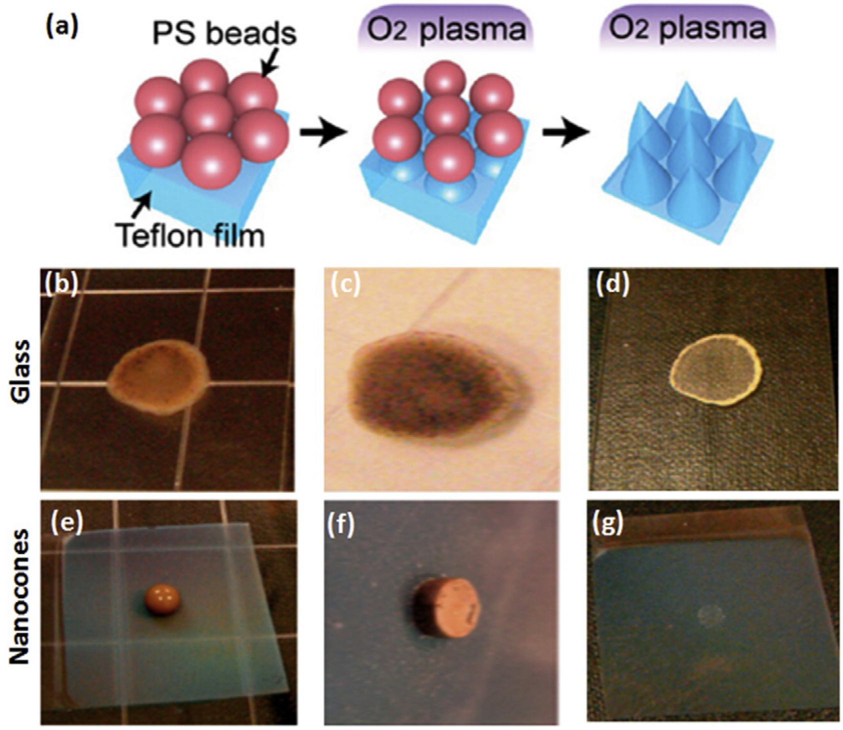

Fig. 7. Photographs of a droplet of muddy water on a hydrophilic glass slide (left column) and on a superhydrophobic surface with nanocone arrays modified with AuNPs and $C_{18}SH$ (right column), (a, d) before and (b, e) after drying, and (c, f) after rinsing with water.

3.2.1. Sol–gel

Sol–gel [86,87] method refers to that, under the condition of acid or alkali, the precursors of chemically active compounds hydrolyze and produce active hydroxyl, then form sol through hydrolytic condensation reaction, and finally become dry gel after concentrating, aging and drying. It should be indicated that after the removal of solvent, some slight nano-pores maybe emerged, which gives some material performance such as superhydrophobicity. [88] SiO_2, TiO_2 and Al_2O_3 are widely used in preparation of superhydrophobic surface via sol–gel method. [64,89,90] Minani et al. [91] prepared alumina gel films on glass plates by sol–gel method. After immersing these films in boiling water, the flower-like porous alumina thin films could be obtained within 30s. Then a superhydrophobic and transparent film with water contact angle of 165° was created, followed by fluoroalkylsilane modification. The roughness of the films increased when the immersing time increased.

Using a hybrid method–a combination of sol–gel-based nano-imprint lithography and hydrothermal growth(as shown in Fig. 11), Lee [55] fabricated TiO_2 hierarchical structures, which have the contact angles over 160° for water. And when water was dropped onto and rolled off the surface, silica nanoparticles on this surface stuck to the liquid droplets and were eliminated from the glass surface. This result confirms the self-cleaning effect of it.

Du [56] successfully fabricated a three-dimensional hierarchical ZnO film via a biomimetic route combining sol–gel technique, soft lithography and hydrothermal treatments. The fabrication process is shown in Fig. 12. A PDMS mold replicated from a fresh lotus leaf was used to imprint microscale pillar structures directly into a ZnO sol film. Hierarchical ZnO micro-/nanostructures were subsequently fabricated by a low-temperature hydrothermal growth of secondary ZnO nanorod arrays on the micro-structured ZnO film. After a low-surface-energy fluoroalkylsilane modification, the film shows the superhydrophobic and self-cleaning properties of lotus leaf.

This approach is simple, mild and low-costing. Moreover, sol–gel technique can realize rapid preparation in large scale, and the request to the base materials is not high. However, the process is very slow and may need several hours and even several days. The structure is not accurate controllable and has a low mechanical strength and solvent contamination. These shortcomings greatly limit their application in preparation of superhydrophobic and self-cleaning surfaces.

3.2.2. Dip coating

Ebert and Bhushan [92] used a simple dip coating method. They created transparent superhydrophobic coatings on glass, polycarbonate and poly(methyl methacrylate) (PMMA) substrates using surface

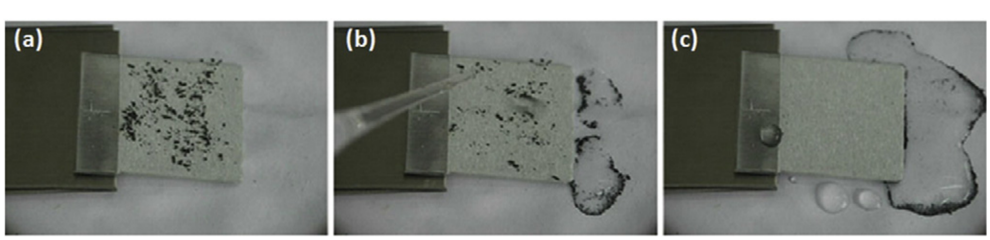

Fig. 8. Self-cleaning effect of the superhydrophobic surfaces on aluminum substrates: (a) graphite powder spreading on the surface, (b) a water droplet rolling through the surface, (c) the aluminum surface being cleaned.

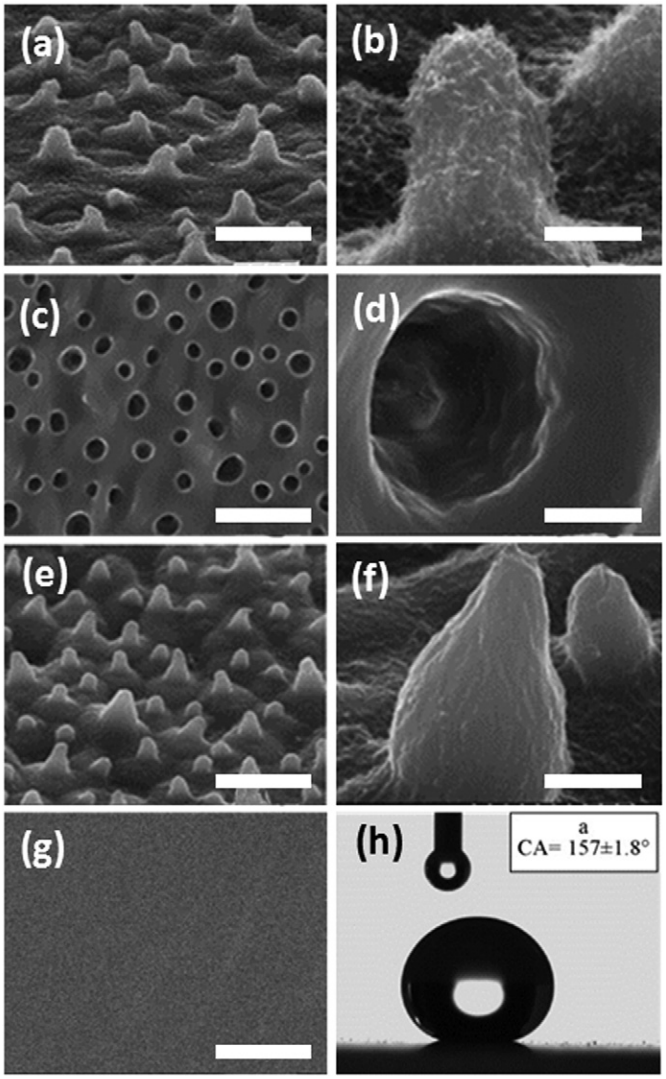

Fig. 9. SEM images of (a) the fresh natural lotus leaf, (b) a single magnified papilla on the fresh natural lotus leaf, (c) the PDMS negative template, (d) a single magnified hole on the PDMS negative template, (e) the lotus-leaf-like super-hydrophobic PVC film, (f) a single magnified papilla on the lotus-leaf-like PVC film, (g) the microscope of smooth PVC film, and (h) water droplets on the as-prepared super-hydrophobic lotus-leaf-like PVC film. (Scale bar: (a, c and e) 20 μm, (b, d and f) 3 μm, (g) 2 μm).

functionalized silica, zinc oxide and indium tin oxide (ITO) nanoparticles in a methylphenyl silicone binder(as shown in Fig. 13).

Yang et al. [93] prepared a durable PTFE superhydrophobic film by the method shown in Fig. 14a, introducing $ZnAc_2$ and NaCl into a commercially available PTFE emulsion. On drying, baking and washing with acetic acid, the PTFE film produced from the emulsion had both micro- and nanoscale surface porosities, and demonstrated superhydrophobic properties, with a static contact angle >150° and a slide angle <10°.

Parkin [94] used many different coating methods to create the water-repellent surfaces, including an artist's spray-gun to coat hard substrates such as glass and steel, dip-coating for cotton wool, and a syringe to extrude the paint onto filter paper. Water droplets tend to bounce instead of wetting the surface, indicating that the surfaces were superhydrophobic. During the self-cleaning tests of the surfaces after oil (hexadecane) contamination, water droplets still formed "marbles" on the dip-coated surface (as shown in Fig. 14b), thus indicating that the surfaces will retain their self-cleaning properties after being contaminated.

3.2.3. Electrochemical deposition

Electrochemical deposition [47,95] has been extensively employed to construct biomimetic superhydrophobic surfaces since it is a versatile technique to prepare microscale and nanoscale structures.

Jiang et al. [96] used an electrochemical deposition method to deposit Au clusters on conductive ITO glass substrate modified with polyelectrolyte multilayer. The clusters exhibit an interesting dendritic structure with nanoscale protuberances, which is a typical hierarchical lotus-like structure. Although the as-prepared film is very hydrophilic, it exhibits superhydrophobicity after being immersed in an ethanol solution of n-dodecanethiol. The CA on the surface is about 156°. It changes to a larger value of ~173° after a 40 min exposure to ambient atmosphere, indicating a good stability of the superhydrophobicity. Similar to the lotus leaf, such surface also shows a small SA of about 1.5°.

3.2.4. Electrostatic spinning

Electrostatic spinning [8,78,97–99] method is the technology for the preparation of micro-/nanofiber developed in recent years. It can obtain polymer fiber with different morphology by controlling the ratio or concentration of spinning solution. Thus, this method is widely used in, and especially suitable for large scale preparation of superhydrophobic surfaces.

Ding et al. [100] reported superhydrophobic surfaces with ZnO nanostructures obtained via electro-spinning. Before FAS coating, the fibrous ZnO films were superhydrophilic, showing a water contact angle of 0°. After FAS coating, however, the fibrous FAS coated ZnO (FZnO) films showed apparent superhydrophobicity with a water contact angle up to 165° and a sliding angle down to 5°.

Jiang and Zhao et al. [4] prepared a bio-lotus-leaf self-cleaning superhydrophobic film with a novel composite structure consisting of porous microspheres and nanofibers. The porous microspheres contributed to the superhydrophobicity by increasing the surface roughness; while nanofibers interweaved to form a 3D network, binding the porous micropheres, which reinforced the composite film. Besides, PS films with different morphology could be obtained by adjusting the concentration of the starting solution. This method proposed a novel effective method for low-cost, large-scale preparation of self-cleaning surface. In another study, Jiang's group [101] reported the preparation of self-cleaning superhydrophobic polyaniline/polystyrene composite films which showed the similar lotus leaf-like micro/nanostructure by a simple electrospinning method. The prepared film exhibited a network of nanofibers with many sub-micrometer-sized spheres distributed on the substrate (Fig. 15a). A higher magnification image (Fig. 15b) shows that the rough micro/nanostructure is composed of many 'nanoknots' connecting the nanofibers together, as well as many nanoscale bumps observed on each sub-microsphere.

3.2.5. Self-assembly

Self-assembly [61,102–107] is another simple and inexpensive method to prepare micro- and nano- dual-scale superhydrophobic surface structures with self-cleaning property, as well as the obtained structures can be finely controlled. For example, Jiang et al. [108] prepared a conducting and superhydrophobic rambutan-like hollow spheres of polyaniline (Fig. 16a) by means of a self-assembly method in the presence of perfluorooctane sulfonic acid (PFOSA), which is employed as a dopant and soft template. The water sphere formed on a surface composed of the rambutan-like hollow spheres has a CA as high as 162.5°, (Fig. 16b) which reveals the superhydrophobic nature of the material. Importantly, the hollow spheres float on the surface of the water, and remain floating for several months because of their hollow and superhydrophobic characteristics. Xin et al. [109] fabricated an artificial lotus leaf structure on cotton substrates via the controlled assembly of carbon nanotubes, which have been endowed with superhydrophobic properties –water contact angles greater than 150°.

As shown in Fig. 16c-f, Zheng et al. [110] used a layer-by-layer (LBL) assembly method to create a novel poly(vinylpyrrolodone)/

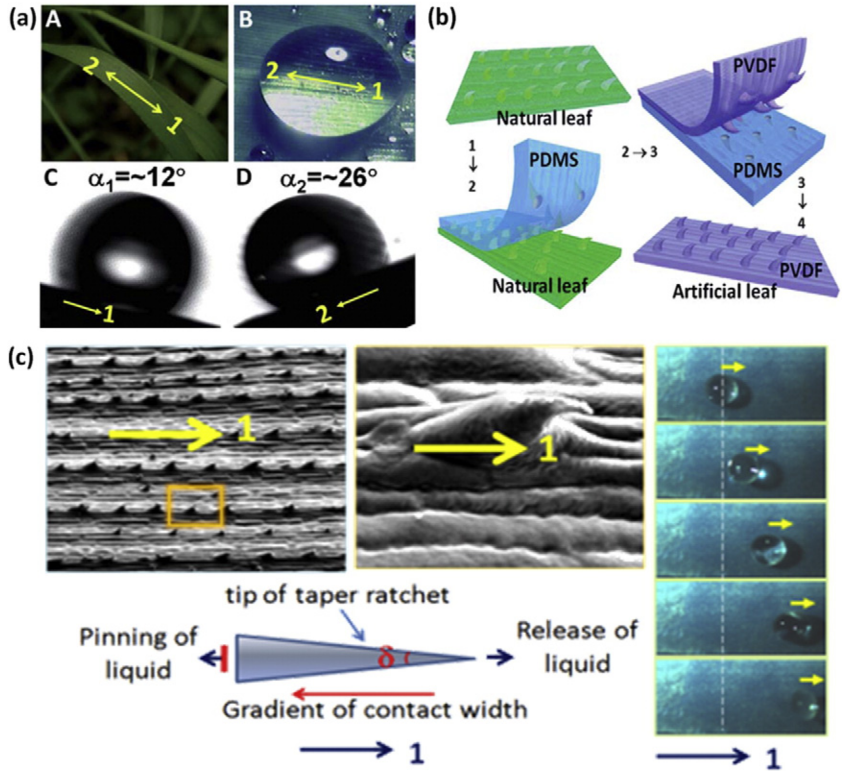

Fig. 10. (a) Photos of fresh ryegrass leaf and a condensed drop on it, (b) illustration of artificial structured surface fabrication process, (c) the micro-structure of artificial structured surface and observation of unidirectional shedding-off of water on it.

poly(urushiol)-CuS multilayer micro- and nanoscale hierarchical superhydrophobic film with a water contact angle of 152°.

3.2.6. Gas (chemical/physical) vapor deposition

By making use of chemical vapor deposition (CVD) technique, Jiang Lei et al. [111–113] fabricated a lotus-like ACNT film on a silica substrate with heterogeneous catalyst distribution. The CA on its surface is about 166°, and the SA is as low as about 3°, which should be attributed to the arrays of nanostructure and microstructure on the surface. Lau et al. [114] fabricated a stable superhydrophobic surface via synthesized carbon nanotube (CNT) template by chemical vapor deposition on a Fe-N catalyst layer and then aligned CNTs coated with a zinc oxide (ZnO) thin film. Contact angle measurement reveals that the surface of the ZnO-coated CNTs is superhydrophobic with water contact angle of 159°. Teare et al. [115] synthesized a low surface energy super-hydrophobic film on the glass substrate via deposition of the 1 H,1 H,2 H,2 H-perfluorooctyl acrylate ($H_2C=CHCO_2CH_2CH_2(CF_2)_5CF_3$, PFAC) plasma polymer. Because of the deposition of well-defined polymeric nanospheres spread on the film, the water contact angle is about 168° and rolling angle is less than 5°, indicating perfect self-cleaning and superhydrophobic performances. Lau et al. [116] created a stable, superhydrophobic surface using the nanoscale roughness inherent in a vertically aligned carbon nanotube forest together with a thin, conformal hydrophobic poly(tetrafluoroethylene) (PTFE) coating on the surface of the nanotubes. The water contact angle on this surface is up to 170°, and it also has a good self-cleaning ability. Jiang et al. [117] fabricated a

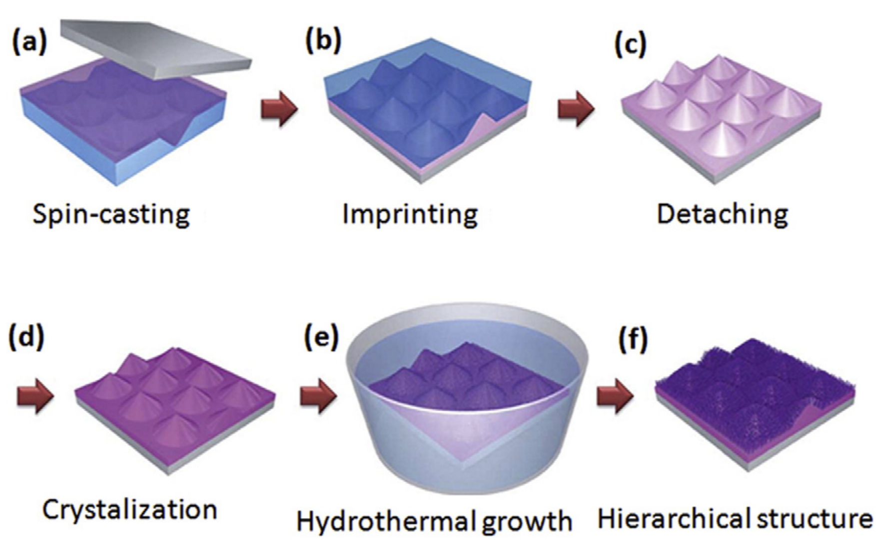

Fig. 11. Schematic illustration of the fabrication process of TiO_2 hierarchical structures along with sol–gel-based nanoimprint lithography and hydrothermal growth.

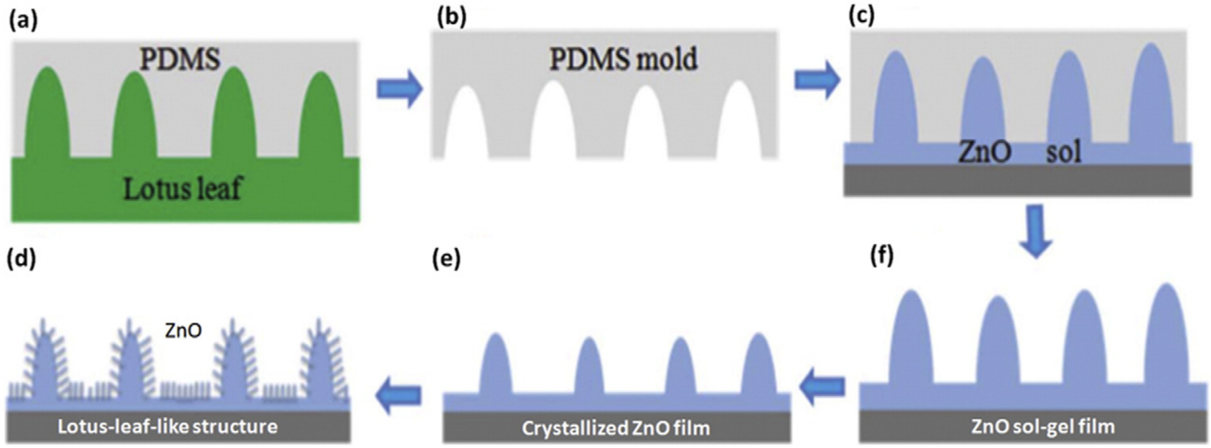

Fig. 12. Schematic representation of the fabrication process of lotus-leaf-like ZnO structures: (a) PDMS replication of fresh lotus leaf, (b) replicated PDMS mold (c) soft imprint on ZnO sol film, (d) imprinted ZnO sol–gel film, (e) crystallized ZnO film after calcination, (f) lotus-leaf-like ZnO micro-/nanostructures after hydrothermal reaction.

superhydrophobic ZnO thin film by the Au-catalyzed chemical vapor deposition method. The surface of the film exhibits hierarchical structure with nanostructures on sub-microstructures. The film was attached tightly to the substrate, showing good stability and durability. And the water contact angle (CA) was 164.3°.

Taking candle soot as a template, Guan et al. [118] created a robust and antireflective polydimethylsiloxane (PDMS) superhydrophobic surface by the technique of CVD at a high temperature. Because of no organic solutions or chemical modification, this scheme is environmentally friendly and efficient method. Though a CVD process at a high temperature, the candle soot template is oxidized and porous structures is easily obtained without damaging the low surface energy. The surfaces with 7.2 mg PDMS have a WCA of 157° and a SA of 3°, as well as a ~ 1.2% higher average transmittance than the bare glass slides in the visible range (400-800 nm). This result is very ideal compared to the other reported similar template methods. [119–122] The photographs of candle soot coated glass and antireflective superhydrophobic glass prepared by CVD of PDMS were shown in Fig. 17. Compared to candle soot (Fig. 17b) that has a diameter of ~60 nm, the CVD particles prepared with 7.2 mg cured PDMS have a smaller size of ~30 nm (Fig. 17e) and the thickness decrease from ~20 mm to less than 300 nm. What is more is that, the candle soot coated surfaces after CVD of PDMS at 370 °C could keep the superhydrophobicity even after the soot removed by water flow impact, meaning the adhesive force of the surfaces was enhanced and chemical bonds have been formed among the CVD particles and between the slides and CVD particles.

Although, the operation process of this method is simple and the binding force between film and substrate is stronger, its high cost limit it only suitable for fabrication of some special materials.

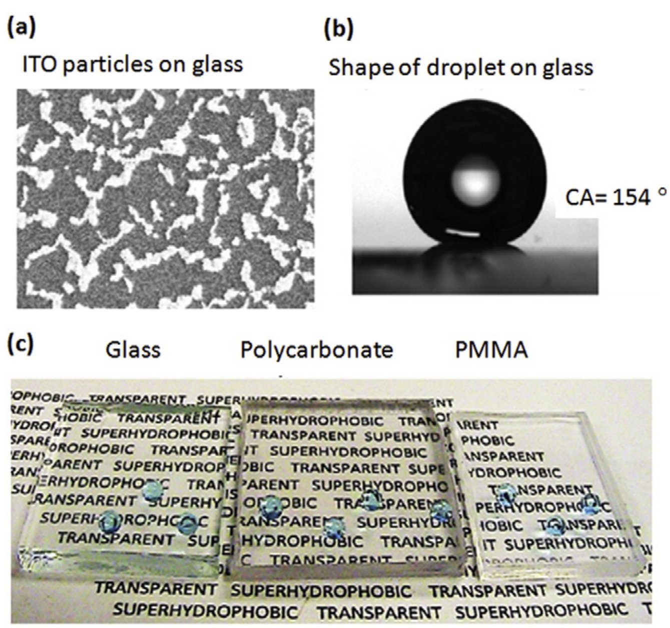

Fig. 13. (a) SEM micrograph of ITO nanoparticle coatings on glass substrates, and (b) water droplets deposited on glass, polycarbonate, and PMMA with ITO nanoparticulate coatings exhibiting superhydrophobicity and high visible transmittance. (Scale bar: (a) 10 μm).

4. Conclusions

In conclusion, both of multi-scale roughness and low energy waxes are responsible to the superhydrophobic and self-cleaning properties of bio-lotus-leaf surfaces. It is clear that the intrinsic hierarchical rough structure is a more essential role of them. In addition, the nanoscale hair-like structure plays a more important role in the aspect of self-cleaning property of the lotus leaf. And then we briefly summarized and discussed the conventional self-cleaning methods. We categorize recent progress in this area into two aspects as the technologies of constructing hierarchical roughness structure onto the hydrophobic surfaces and the technologies of coating low energy materials onto the rough surfaces.

Enormous amounts of researches on superhydrophobic self-cleaning surfaces based on the surface micro/nanomorphologies of bio-inspired lotus leaf have been successfully carried out on the small scale in the laboratory. And numbers of self-cleaning products have been commercialized in fields of self-cleaning windows, windshields, exterior paints for buildings and navigation of ships, utensils, roof tiles, textiles, solar panels, and applications requiring a reduction of drag in fluid flow, e.g., in micro/nanochannels. However, such surfaces are mechanically weak and even stop functioning when exposed to oil. They would be ineffective when applied on the large scale due to several reasons. Therefore, further research for the preparation methods is needed to obtain superhydrophobic surfaces with better self-cleaning performance. We hope that this review article should provide a useful guide for the development of self-cleaning surfaces.

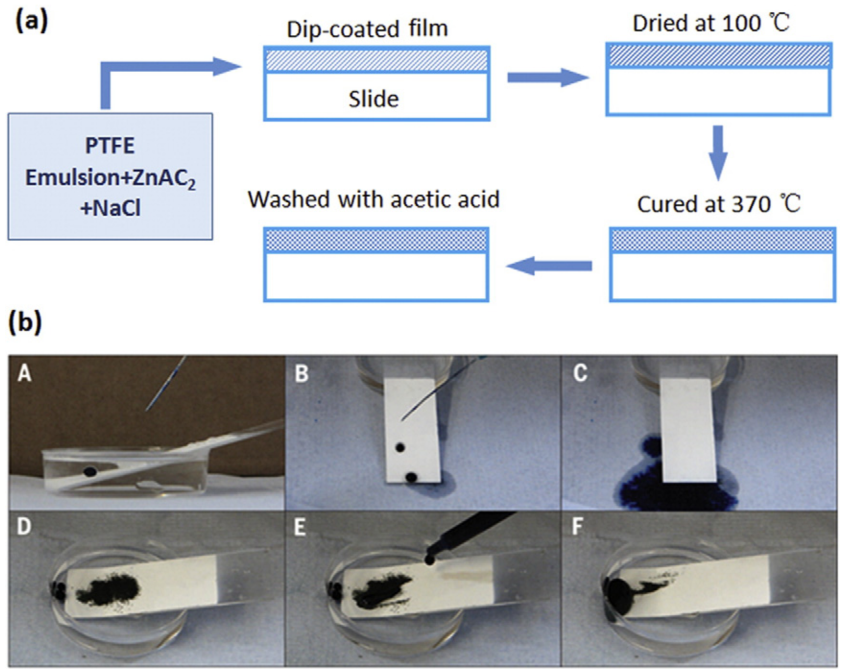

Fig. 14. (a) A schematic of superhydrophobic PTFE film preparation, (b) Self-cleaning tests after oil-contaminations of the surface.

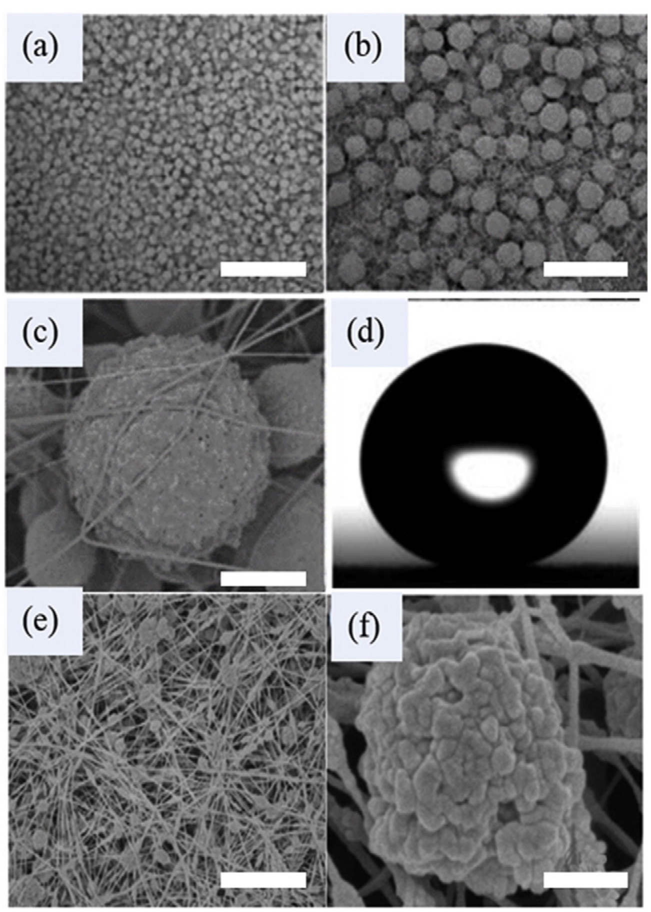

Fig. 15. Composite PS films prepared by electrohydrodynamics (EHD) technique. (a)-(c): SEM images of the prepared PS films. (d) Water droplet on the film (CA = 160.4°). (e) SEM image of an electrospun PANI/PS composite film with lotus-leaf-like structure prepared from a 3.72 wt.% PS: ABSA/DMF solution; (f) Magnified view of a single sub-microsphere from (e). (Scale bar: (a-b) 10 μm, (c and e) 1 μm (f) 100 nm).

Acknowledgements

This work is supported by National Research Fund for Fundamental Key Project (2013CB933001), National Natural Science Foundation of China (21234001, 21473007), Doctoral Fund of Ministry of Education of China (20121102110035).

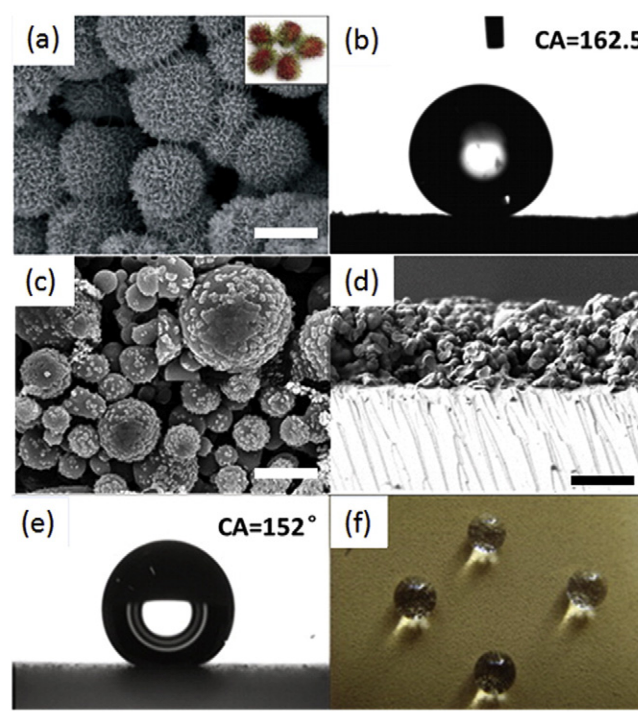

Fig. 16. (a) SEM image of the rambutan-like hollow PANI spheres, inset: a photograph of a rambutan, b) Shape of a water droplet on a surface of the rambutan-like PANI hollow spheres; (c) SEM images of the superhydrophobic $(PVP/PU\text{-}CuS)_8$ film. Inset: magnified view of PU-CuS particles in (c), (d) The cross-sectional SEM image of the superhydrophobic $(PVP/PU\text{-}CuS)_8$ film, (e)the CA of water on the $(PVP/PU\text{-}CuS)_8$ film, and (f) some water droplets on the $(PVP/PU\text{-}CuS)_8$ film. (Scale bar: (a) 100 nm, (c-d) 1 μm).

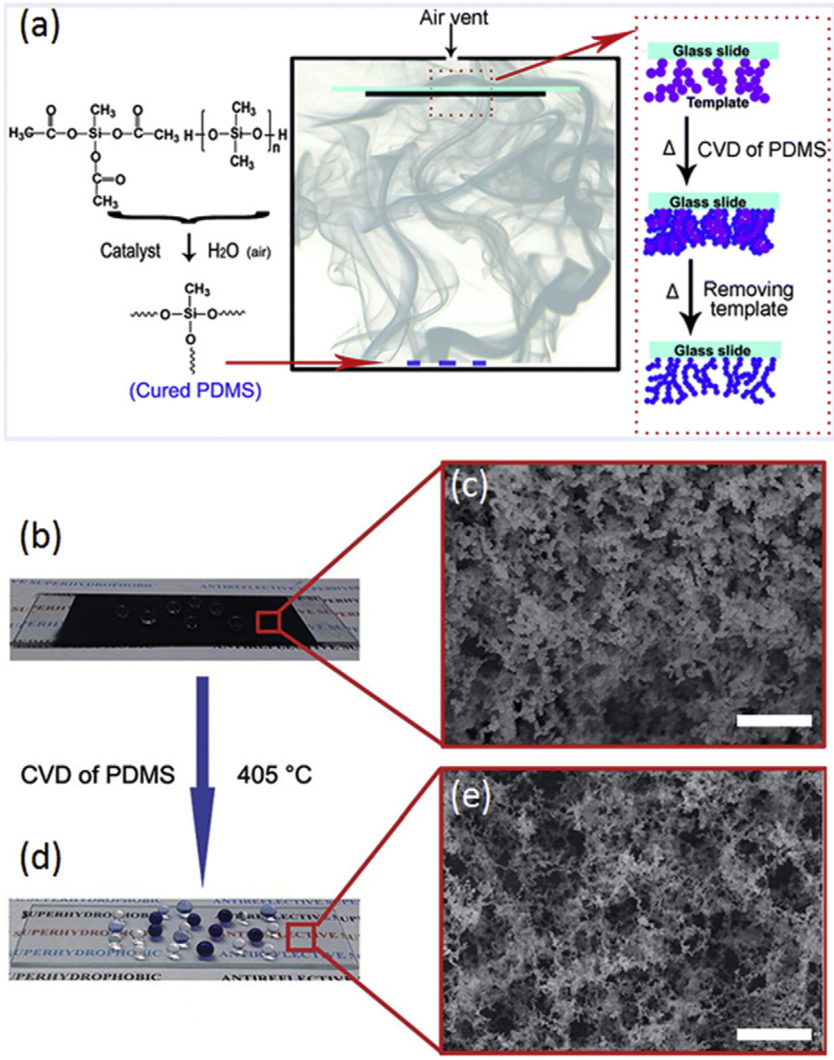

Fig. 17. (a) Schematic illustration for preparing the superhydrophobic Surfaces, (b and d) photographs of the candle soot coated glass and antireflective superhydrophobic glass prepared by CVD of 7.2 mg cured PDMS, on which water droplets and ink droplets deposited, and (c, e) SEM images of the candle soot, the superhydrophobic surfaces prepared by CVD of 7.2 and 9.2 mg cured PDMS. (Scale bar: (c) and (e) 1 μm).

References

[1] M. Nosonovsky, B. Bhushan, Patterned nonadhesive surfaces: superhydrophobicity and wetting regime transitions, Langmuir 24 (2008) 1525–1533.

[2] W. Barthlott, C. Neinhuis, Purity of the sacred lotus, or escape from contamination in biological surfaces, Planta 202 (1997) 1–8.

[3] C. Neinhuis, W. Barthlott, Characterization and distribution of water-repellent, Self Clean Plant Surf Ann Bot 79 (1997) 667–677.

[4] L. Jiang, Y. Zhao, J. Zhai, A lotus-leaf-like superhydrophobic surface: a porous microsphere/nanofiber composite film prepared by electrohydrodynamics, Angew Chem Int Ed 43 (2004) 4338–4341.

[5] D. Deng, J.Y. Lee, Direct fabrication of double-rough chestnut-like multifunctional Sn@C composites on copper foil: lotus effect and lithium ion storage properties, J Mater Chem 20 (2010) 8045.

[6] Z. Guo, W. Liu, B.L. Su, Superhydrophobic surfaces: from natural to biomimetic to functional, J Colloid Interface Sci 353 (2011) 335–355.

[7] C. Frankiewicz, F. Zoueshtiagh, A. Talbi, J. Streque, P. Pernod, A. Merlen, From 'petal effect' to 'lotus effect' on the highly flexible silastic S elastomer microstructured using a fluorine based reactive ion etching process, J Micromech Microeng 24 (2014) 115008.

[8] S.S. Latthe, C. Terashima, K. Nakata, A. Fujishima, Superhydrophobic surfaces developed by mimicking hierarchical surface morphology of lotus leaf, Molecules 19 (2014) 4256–4283.

[9] Y. Zheng, D. Han, J. Zhai, L. Jiang, In situ investigation on dynamic suspending of microdroplet on lotus leaf and gradient of wettable micro- and nanostructure from water condensation, Appl Phys Lett 92 (2008) 084106.

[10] S. Lee, J.H. Kang, S.J. Lee, W. Hwang, Tens of centimeter-scale flexible superhydrophobic nanofiber structures through curing process, Lab Chip 9 (2009) 2234–2237.

[11] E. Celia, T. Darmanin, E. Taffin de Givenchy, S. amigoni, F. guittard, Recent advances in designing superhydrophobic surfaces, J Colloid Interface Sci 402 (2013) 1–18.

[12] J. Chen, R. Dou, D. Cui, Q. Zhang, Y. Zhang, F. Xu, et al., Robust prototypical anti-icing coatings with a self-lubricating liquid water layer between ice and substrate, ACS Appl Mater Interfaces 5 (2013) 4026–4030.

[13] Y. Li, G. Duan, G. Liu, W. Cai, Physical processes-aided periodic micro/nanostructured arrays by colloidal template technique: fabrication and applications, Chem Soc Rev 42 (2013) 3614–3627.

[14] G.D. Bixler, A. Theiss, B. Bhushan, S.C. Lee, Anti-fouling properties of microstructured surfaces bio-inspired by rice leaves and butterfly wings, J Colloid Interface Sci 419 (2014) 114–133.

[15] I.P. Parkin, R.G. Palgrave, Self-cleaning coatings, J Mater Chem 15 (2005) 1689.

[16] V.A. Ganesh, H.K. Raut, A.S. Nair, S. Ramakrishna, A review on self-cleaning coatings, J Mater Chem 21 (2011) 16304.

[17] B. Bhushan, Bioinspired structured surfaces, Langmuir 28 (2012) 1698–1714.

[18] R. Blossey, Self-cleaning surfaces [mdash] virtual realities, Nat Mater 2 (2003) 301–306.

[19] D.H. Kwon, H.K. Huh, S.J. Lee, Wettability and impact dynamics of water droplets on rice (Oryza sativa L.) leaves, Exp Fluids 55 (1691) (2014) 470–479.

[20] G.D. Bixler, B. Bhushan, Bioinspired rice leaf and butterfly wing surface structures combining shark skin and lotus effects, Soft Matter 8 (2012) 11271–11284.

[21] M.J. Mayser, H.F. Bohn, M. Reker, W. Barthlott, Measuring air layer volumes retained by submerged floating-ferns salvinia and biomimetic superhydrophobic surfaces, Beilstein J Nanotechnol (2014) 812–821.

[22] W. Barthlott, T. Schimmel, S. Wiersch, K. Koch, M. Brede, M. Barczewski, et al., The salvinia paradox: superhydrophobic surfaces with hydrophilic pins for air retention under water, Adv Mater 22 (2010) 2325–2328.

[23] Y.Y. Yan, N. Gao, W. Barthlott, Mimicking natural superhydrophobic surfaces and grasping the wetting process: a review on recent progress in preparing superhydrophobic surfaces, Adv Colloid Interface Sci 169 (2011) 80–105.

[24] X. Gao, X. Yan, X. Yao, L. Xu, K. Zhang, J. Zhang, et al., The dry-style antifogging properties of mosquito compound eyes and artificial analogues prepared by soft lithography, Adv Mater 19 (2007) 2213–2217.
[25] L. Feng, S. Li, Y. Li, H. Li, L. Zhang, J. Zhai, et al., Super-hydrophobic surfaces: from natural to artificial, Adv Mater 14 (2002) 1857–1860.
[26] A.B.D. Cassie, S. Baxter, Wettability of porous surfaces, Trans Faraday Soc 40 (1944) 546–551.
[27] D. Quéré, A. Lafuma, J. Bico, Slippy and sticky microtextured solids, Nanotechnology 14 (2003) 1109.
[28] N.A. Patankar, Mimicking the lotus effect: influence of double roughness structures and slender pillars, Langmuir 20 (2004) 8209–8213.
[29] Y.T. Cheng, D.E. Rodak, C.A. Wong, C.A. Hayden, Effects of micro- and Nano-structures on the self-cleaning behaviour of lotus leaves, Nanotechnology 17 (2006) 1359–1362.
[30] P. Wagner, R. Fürstner, W. Barthlott, C. Neinhuis, Quantitative assessment to the structural basis of water repellency in natural and technical surfaces, J Exp Bot 54 (2003) 1295–1303.
[31] S.C. Walker, S. Allen, G. Bell, C.J. Roberts, Analysis of leaf surfaces using scanning ion conductance microscopy, J Microsc 258 (2015) 119–126.
[32] H. Bargel, K. Koch, Z. Cerman, C. Neinhuis, Evans review no. 3: structure–function relationships of the plant cuticle and cuticular waxes – a smart material? Funct Plant Biol 33 (2006) 893–910.
[33] W. Barthlott, C. Neinhuis, D. Cutler, F. Ditsch, I. Meusel, I. Theisen, et al., Classification and terminology of plant epicuticular waxes, Bot J Linn Soc 126 (1998) 237–260.
[34] B. Bhushan, J.Y. Chae, Wetting study of patterned surfaces for superhydrophobicity, Ultramicroscopy 107 (2007) 1033–1041.
[35] B. Bhushan, Y.C. Jung, Wetting, adhesion and friction of superhydrophobic and hydrophilic leaves and fabricated micro/nanopatterned surfaces, J Phys Condens Matter 20 (2008) 225010.
[36] R. Fürstner, W. Barthlott, C. Neinhuis, P. Walzel, Wetting and self-cleaning properties of artificial superhydrophobic surfaces, Langmuir 21 (2005) 956–961.
[37] E. Hosono, S. Fujihara, I. Honma, H. Zhou, Superhydrophobic perpendicular nanopin film by the bottom-up process, J Am Chem Soc 127 (2005) 13458–13459.
[38] M. Karlsson, P. Forsberg, F. Nikolajeff, From hydrophilic to superhydrophobic: fabrication of micrometer-sized nail-head-shaped pillars in diamond, Langmuir 26 (2010) 889–893.
[39] L. Cao, H.-H. Hu, D. Gao, Design and fabrication of micro-textures for inducing a superhydrophobic behavior on hydrophilic materials, Langmuir 23 (2007) 4310–4314.
[40] G.D. Bixler, B. Bhushan, Fluid drag reduction and efficient self-cleaning with rice leaf and butterfly wing bioinspired surfaces, NanoscaleNanoscale. 5 (2013) 7685–7710.
[41] K. Liu, X. Yao, L. Jiang, Recent developments in bio-inspired special wettability, Chem Soc Rev 39 (2010) 3240–3255.
[42] V. Mortazavi, M. Nosonovsky, Wear-induced microtopography evolution and wetting properties of self-cleaning, lubricating and healing surfaces, J Adhes Sci Technol 25 (2012) 1337–1359.
[43] T. Verho, C. Bower, P. Andrew, S. Franssila, O. Ikkala, R.H. Ras, Mechanically durable superhydrophobic surfaces, Adv Mater 23 (2011) 673–678.
[44] D. Xia, L.M. Johnson, G.P. Lopez, Anisotropic wetting surfaces with one-dimensional and directional structures: fabrication approaches, wetting properties and potential applications, Adv Mater 24 (2012) 1287–1302.
[45] Z. Cheng, M. Du, H. Lai, N. Zhang, K. Sun, From petal effect to lotus effect: a facile solution immersion process for the fabrication of super-hydrophobic surfaces with controlled adhesion, NanoscaleNanoscale 5 (2013) 2776–2783.
[46] A. Tuteja, W. Choi, M. Ma, J.M. Mabry, S.A. Mazzella, G.C. Rutledge, et al., Designing superoleophobic surfaces, Science 318 (2007) 1618–1622.
[47] H.A. Burgoyne, P. Kim, M. Kolle, A.K. Epstein, J. Aizenberg, Screening conditions for rationally engineered electrodeposition of nanostructures (SCREEN): electrodeposition and applications of polypyrrole nanofibers using microfluidic gradients, Small 8 (2012) 3502–3509.
[48] X. Feng, Y. Shi, Y. Wang, G. Yue, W. Yang, Preparation of superhydrophobic silver Nano coatings with feather-like structures by electroless galvanic deposition, Chin Sci Bull 58 (2013) 1887–1891.
[49] B. Hatton, V. Kitaev, D. Perovic, G. Ozin, J. Aizenberg, Low-temperature synthesis of nanoscale silica multilayers – atomic layer deposition in a test tube, J Mater Chem 20 (2010) 6009.
[50] B.D. Hatton, J. Aizenberg, Writing on superhydrophobic nanopost arrays: topographic design for bottom-up assembly, Nano Lett 12 (2012) 4551–4557.
[51] P. Kim, A.K. Epstein, M. Khan, L.D. Zarzar, D.J. Lipomi, G.M. Whitesides, et al., Structural transformation by electrodeposition on patterned substrates (STEPS): a new versatile nanofabrication method, Nano Lett 12 (2012) 527–533.
[52] L. Li, V. Breedveld, D.W. Hess, Design and fabrication of superamphiphobic paper surfaces, ACS Appl Mater Interfaces 5 (2013) 5381–5386.
[53] S. Tawfick, M. De Volder, D. Copic, S.J. Park, C.R. Oliver, E.S. Polsen, et al., Engineering of micro- and nanostructured surfaces with anisotropic geometries and properties, Adv Mater 24 (2012) 1628–1674.
[54] X. Wang, R.A. Weiss, A facile method for preparing sticky, hydrophobic polymer surfaces, Langmuir 28 (2012) 3298–3305.
[55] H.-J. Choi, J.-H. Shin, S. Choo, J. Kim, H. Lee, A tunable method for nonwetting surfaces based on nanoimprint lithography and hydrothermal growth, J Mater Chem A 1 (2013) 8417.
[56] S. Dai, D. Zhang, Q. Shi, X. Han, S. Wang, Z. Du, Biomimetic fabrication and tunable wetting properties of three-dimensional hierarchical ZnO structures by combining soft lithography templated with lotus leaf and hydrothermal treatments, CrystEngComm 15 (2013) 5417.
[57] S.H. Kang, N. Wu, A. Grinthal, J. Aizenberg, Meniscus lithography: evaporation-induced self-organization of pillar arrays into moiré patterns, Phys Rev Lett 107 (2011).
[58] P. Kim, W.E. Adorno-Martinez, M. Khan, J. Aizenberg, Enriching libraries of high-aspect-ratio micro- or nanostructures by rapid, low-cost, benchtop nanofabrication, Nat Protoc 7 (2012) 311–327.
[59] N.E. Kurland, T. Dey, C. Wang, S.C. Kundu, V.K. Yadavalli, Silk protein lithography as a route to fabricate sericin microarchitectures, Adv Mater 26 (2014) 4431–4437.
[60] S.Y. Min, T.S. Kim, B.J. Kim, H. Cho, Y.Y. Noh, H. Yang, et al., Large-scale organic nanowire lithography and electronics, Nat Commun 4 (2013) 1773.
[61] J.G. Son, A.F. Hannon, K.W. Gotrik, A. Alexander-Katz, C.A. Ross, Hierarchical nanostructures by sequential self-assembly of styrene-dimethylsiloxane block copolymers of different periods, Adv Mater 23 (2011) 634–639.
[62] B. Bhushan, Y.C. Jung, Natural and biomimetic artificial surfaces for superhydrophobicity, self-cleaning, low adhesion, and drag reduction, Prog Mater Sci 56 (2011) 1–108.
[63] J. Liu, Z. Liu, T. Zhang, J. Zhai, L. Jiang, Low-temperature crystallization of anodized TiO2 nanotubes at the solid-gas interface and their photoelectrochemical properties, NanoscaleNanoscale. 5 (2013) 6139–6144.
[64] J. Dong, X. Ouyang, J. Han, W. Qiu, W. Gao, Superhydrophobic surface of TiO2 hierarchical nanostructures fabricated by Ti anodization, J Colloid Interface Sci 420 (2014) 97–100.
[65] C. Jeong, C.-H. Choi, Single-step direct fabrication of pillar-on-pore hybrid nanostructures in anodizing aluminum for superior superhydrophobic efficiency, ACS Appl Mater Interfaces 4 (2012) 842–848.
[66] C. Guo, L. Feng, J. Zhai, G. Wang, Y. Song, L. Jiang, et al., Large-area fabrication of a nanostructure-induced hydrophobic surface from a hydrophilic polymer, Chemphyschem 5 (2004) 750–753.
[67] Y. Kim, S. Lee, H. Cho, B. Park, D. Kim, W. Hwang, Robust superhydrophilic/hydrophobic surface based on self-aggregated Al2O3 nanowires by single-step anodization and self-assembly method, ACS Appl Mater Interfaces 4 (2012) 5074–5078.
[68] P. Chevallier, S. Turgeon, C. Sarra-Bournet, R. Turcotte, G. Laroche, Characterization of multilayer anti-fog coatings, ACS Appl Mater Interfaces 3 (2011) 750–758.
[69] X. Han, L. Wang, X. Wang, Fabrication of chemical gradient using space limited plasma oxidation and its application for droplet motion, Adv Funct Mater 22 (2012) 4533–4538.
[70] B.S. Yilbas, Laser treatment of zirconia surface for improved surface hydrophobicity, J Alloys Compd 625 (2015) 208–215.
[71] M.R. Cardoso, R.J. Martins, A. Dev, T. Voss, C.R. Mendonca, Highly hydrophobic hierarchical nanomicro roughness polymer surface created by stamping and laser micromachining, J Appl Polym Sci 132 (2015).
[72] M. Ruan, W. Li, B. Wang, B. Deng, F. Ma, Z. Yu, Preparation and anti-icing behavior of superhydrophobic surfaces on aluminum alloy substrates, Langmuir 29 (2013) 8482–8491.
[73] H.D. Yu, M.D. Regulacio, E. Ye, M.Y. Han, Chemical routes to top-down nanofabrication, Chem Soc Rev 42 (2013) 6006–6018.
[74] D.J. Lipomi, R.V. Martinez, M.A. Kats, S.H. Kang, P. Kim, J. Aizenberg, et al., Patterning the tips of optical fibers with metallic nanostructures using nanoskiving, Nano Lett 11 (2011) 632–636.
[75] A.-M. Kietzig, S.G. Hatzikiriakos, P. Englezos, Patterned superhydrophobic metallic surfaces, Langmuir 25 (2009) 4821–4827.
[76] B. Balu, V. Breedveld, D.W. Hess, Fabrication of "roll-off" and "sticky" superhydrophobic cellulose surfaces via plasma processing, Langmuir 24 (2008) 4785–4790.
[77] Y. Kwon, N. Patankar, J. Choi, J. Lee, Design of surface hierarchy for extreme hydrophobicity, Langmuir 25 (2009) 6129–6136.
[78] M. Toma, G. Loget, R.M. Corn, Flexible Teflon nanocone array surfaces with tunable superhydrophobicity for self-cleaning and aqueous droplet patterning, ACS Appl Mater Interfaces 6 (2014) 11110–11117.
[79] J. Song, W. Xu, Y. Lu, One-step electrochemical machining of superhydrophobic surfaces on aluminum substrates, J Mater Sci 47 (2012) 162–168.
[80] Y. Deng, J. Wei, Z. Sun, D. Zhao, Large-pore ordered mesoporous materials templated from non-pluronic amphiphilic block copolymers, Chem Soc Rev 42 (2013) 4054–4070.
[81] D. Losic, Microstructured surfaces engineered using biological templates: a facile approach for the fabrication of superhydrophobic surfaces, J Serb Chem Soc 73 (2008) 1123–1135.
[82] S. Lee, W. Hwang, Ultralow contact angle hysteresis and no-aging effects in superhydrophobic tangled nanofiber structures generated by controlling the pore size of a 99.5% aluminum foil, J Micromech Microeng 19 (2009) 035019.
[83] M. Xu, N. Lu, H. Xu, D. Qi, Y. Wang, S. Shi, et al., Fabrication of flexible superhydrophobic biomimic surfaces, Soft Matter 6 (2010) 1438–1443.
[84] Z. Yuan, H. Chen, J. Zhang, Facile method to prepare lotus-leaf-like superhydrophobic poly(vinyl chloride) film, Appl Surf Sci 254 (2008) 1593–1598.
[85] P. Guo, Y. Zheng, C. Liu, J. Ju, L. Jiang, Directional shedding-off of water on natural/bio-mimetic taper-ratchet array surfaces, Soft Matter 8 (2012) 1770–1775.
[86] R. Taurino, E. Fabbri, M. Messori, F. Pilati, D. Pospiech, A. Synytska, Facile preparation of superhydrophobic coatings by sol–gel processes, J Colloid Interface Sci 325 (2008) 149–156.
[87] L. Mishchenko, B. Hatton, M. Kolle, J. Aizenberg, Patterning hierarchy in direct and inverse opal crystals, Small 8 (2012) 1904–1911.
[88] Y.-Y. Zhang, Q. Ge, L.-L. Yang, X.-J. Shi, J.-J. Li, D.-Q. Yang, et al., Durable superhydrophobic PTFE films through the introduction of micro- and nanostructured pores, Appl Surf Sci 339 (2015) 151–157.
[89] B.E. Pinchasik, H. Mohwald, A.G. Skirtach, Mimicking bubble use in nature: propulsion of Janus particles due to hydrophobic-hydrophilic interactions, Small 10 (2014) 2670–2677.

[90] S. Dong, X. Zhang, F. He, S. Dong, D. Zhou, B. Wang, Visible-light photocatalytic degradation of methyl orange over spherical activated carbon-supported and Er3+: YAlO3-doped TiO2in a fluidized bed, J Chem Technol Biotechnol 90 (2015) 880–887.
[91] K. Tadanaga, J. Morinaga, A. Matsuda, T. Minami, Superhydrophobic – superhydrophilic micropatterning on flowerlike alumina coating film by the sol–gel method, Chem Mater 12 (2000) 590–592.
[92] D. Ebert, B. Bhushan, Transparent, superhydrophobic, and wear-resistant coatings on glass and polymer substrates using SiO2, ZnO, and ITO nanoparticles, Langmuir 28 (2012) 11391–11399.
[93] Z. Xia, C. Chen, H. Fang, S. Chen, The mechanism and process of nanosecond pulsed-laser induced subwavelength periodic ripples on silica films, Appl Surf Sci 337 (2015) 151–157.
[94] Y. Lu, S. Sathasivam, J. Song, C.R. Crick, C.J. Carmalt, I.P. Parkin, Repellent materials. Robust self-cleaning surfaces that function when exposed to either air or oil, Science 347 (2015).
[95] Q.L. Sheng, R.X. Liu, J.B. Zheng, J.J. Zhu, Reversible switches of DNA nanostructures between "closed" and "open" states and their biosensing applications, NanoscaleNanoscale. 5 (2013) 7505–7511.
[96] X. Zhang, F. Shi, X. Yu, H. Liu, Y. Fu, Z. Wang, et al., Polyelectrolyte multilayer as matrix for electrochemical deposition of gold clusters: toward super-hydrophobic surface, J Am Chem Soc 126 (2004) 3064–3065.
[97] P. Tan, Multi-scale force-resistant superhydrophobic superoleophobic textile surfaces: North Carolina state university, 2012.
[98] W. Liang, Y. Zhang, B. Wang, Z. Guo, W. Liu, Biological applications of biomimetic superhydrophobic surfaces, Acta Chim Sin 70 (2012) 2393.
[99] B. Wang, J. Li, G. Wang, W. Liang, Y. Zhang, L. Shi, et al., Methodology for robust superhydrophobic fabrics and sponges from in situ growth of transition metal/metal oxide nanocrystals with thiol modification and their applications in oil/water separation, ACS Appl Mater Interfaces 5 (2013) 1827–1839.
[100] B. Ding, T. Ogawa, J. Kim, K. Fujimoto, S. Shiratori, Fabrication of a superhydrophobic nanofibrous zinc oxide film surface by electrospinning, Thin Solid Films 516 (2008) 2495–2501.
[101] Y. Zhu, J. Zhang, Y. Zheng, Z. Huang, L. Feng, L. Jiang, Stable, superhydrophobic, and conductive polyaniline/polystyrene films for corrosive environments, Adv Funct Mater 16 (2006) 568–574.
[102] G. Demirel, F. Buyukserin, Surface-induced self-assembly of dipeptides onto nanotextured surfaces, Langmuir 27 (2011) 12533–12538.
[103] J. Liu, W. Huang, Y. Pang, P. Huang, X. Zhu, Y. Zhou, et al., Molecular self-assembly of a homopolymer: an alternative to fabricate drug-delivery platforms for cancer therapy, Angew Chem 50 (2011) 9162–9166.
[104] T. Marangoni, D. Bonifazi, Nano- and microstructuration of supramolecular materials driven by H-bonded uracil.2,6-diamidopyridine complexes, Nanoscale 5 (2013) 8837–8851.
[105] Y. Rahmawan, L. Xu, S. Yang, Self-assembly of nanostructures towards transparent, superhydrophobic surfaces, J. Mater. Chem. A. 1 (2013) 2955–2969.
[106] I. Ziemecka, G.J.M. Koper, A.G.L. Olive, J.H. van Esch, Chemical-gradient directed self-assembly of hydrogel fibers, Soft Matter 9 (2013) 1556.
[107] R. Daly, O. Kotova, M. Boese, T. Gunnlaugsson, J.J. Boland, Chemical Nano-gardens: growth of salt nanowires from supramolecular self-assembly gels, ACS Nano 7 (2013) 4838–4845.
[108] Y. Zhu, D. Hu, M.X. Wan, L. Jiang, Y. Wei, Conducting and superhydrophobic rambutan-like hollow spheres of polyaniline, Adv Mater 19 (2007) 2092–2096.
[109] Y. Liu, J. Tang, R. Wang, H. Lu, L. Li, Y. Kong, et al., Artificial lotus leaf structures from assembling carbon nanotubes and their applications in hydrophobic textiles, J Mater Chem 17 (2007) 1071–1078.
[110] X.-L. Zheng, J.-B. Weng, B.-H. Hu, X.-Z. Lv, D.-L. Meng, A.S.C. Chan, Fabrication of a stable superhydrophobic film constructed by poly(vinylpyrrolidone)/poly(urushiol)-CuS through layer-by-layer assembly, Mater Chem Phys 130 (2011) 1054–1060.
[111] R. Raj, S.C. Maroo, E.N. Wang, Wettability of graphene, Nano Lett 13 (2013) 1509–1515.
[112] H.H. Kim, Y. Chung, E. Lee, S.K. Lee, K. Cho, Water-free transfer method for CVD-grown graphene and its application to flexible air-stable graphene transistors, Adv Mater 26 (2014) 3213–3217.
[113] T. Sun, L. Feng, X. Gao, L. Jiang, Bioinspired surfaces with special wettability, Acc Chem Res 38 (2005) 644–652.
[114] L. Huang, S.P. Lau, H.Y. Yang, E.S.P. Leong, S.F. Yu, S. Prawer, Stable superhydrophobic surface via carbon nanotubes coated with a ZnO thin film, J Phys Chem B 109 (2005) 7746–7748.
[115] D.O.H. Teare, C.G. Spanos, P. Ridley, E.J. Kinmond, V. Roucoules, J.P.S. Badyal, et al., Pulsed plasma deposition of super-hydrophobic nanospheres, Chem Mater 14 (2002) 4566–4571.
[116] K.K.S. Lau, J. Bico, K.B.K. Teo, M. Chhowalla, G.A.J. Amaratunga, W.I. Milne, et al., Superhydrophobic carbon nanotube forests, Nano Lett 3 (2003) 1701–1705.
[117] H. Liu, L. Feng, J. Zhai, L. Jiang, D. Zhu, Reversible wettability of a chemical vapor deposition prepared ZnO film between superhydrophobicity and superhydrophilicity, Langmuir 20 (2004) 5659–5661.
[118] X. Liu, Y. Xu, Z. Chen, K. Ben, Z. Guan, Robust and antireflective superhydrophobic surfaces prepared by CVD of cured polydimethylsiloxane with candle soot as a template, RSC Adv 5 (2015) 1315–1318.
[119] X. Deng, L. Mammen, Y. Zhao, P. Lellig, K. Müllen, C. Li, et al., Transparent, thermally stable and mechanically robust superhydrophobic surfaces made from porous silica capsules, Adv Mater 23 (2011) 2962–2965.
[120] X. Deng, L. Mammen, H.J. Butt, D. Vollmer, Candle soot as a template for a transparent robust superamphiphobic coating, Science 335 (2012) 67–70.
[121] S. Liu, M. Sakai, B. Liu, C. Terashima, K. Nakata, A. Fujishima, Facile synthesis of transparent superhydrophobic titania coating by using soot as a nanoimprint template, RSC Adv 3 (2013) 22825–22829.
[122] X. Zhu, Z. Zhang, G. Ren, X. Men, B. Ge, X. Zhou, Designing transparent superamphiphobic coatings directed by carbon nanotubes, J Colloid Interface Sci 421 (2014) 141–145.